PHYSICAL REVIEW A **81**, 021402(R) (2010)

Trapping deuterium atoms

A. W. Wiederkehr, S. D. Hogan, B. Lambillotte, M. Andrist, H. Schmutz, J. Agner, Y. Salathé, and F. Merkt
Laboratorium für Physikalische Chemie, ETH Zürich, CH-8093, Switzerland
(Received 22 December 2009; published 24 February 2010)

Cold deuterium atoms in a supersonic beam have been decelerated from an initial velocity of 475 m/s to zero velocity in the laboratory frame using a 24-stage Zeeman decelerator. The atoms have been loaded in a magnetic quadrupole trap at a temperature of ~100 mK and an initial density of $\sim 10^6$ cm^{-3}. Efficient deceleration was achieved by pulsing the magnetic fields in the decelerator solenoids using irregular sequences of phase angles. Trap loading was optimized by monitoring and suppressing the observed reflection of the atoms by the field gradient of the back solenoid of the trap.

DOI: 0.1103/PhysRevA.81.021402 PACS number(s): 37.10.Mn, 32.60.+i

Since the first demonstration of phase-stable multistage deceleration of polar molecules in pulsed supersonic beams using a 63-stage Stark decelerator by Bethlem *et al.* [1,2], multistage deceleration has been established as an important method to produce cold molecules. The method can be used to prepare molecular beams with a mean velocity sufficiently low that subsequent loading in electrostatic [3], electrodynamic [4], and magnetoelectrostatic [5] traps is possible. Multistage Zeeman deceleration, the magnetic analog of multistage Stark deceleration, has recently been developed as one approach to the production of slow beams of paramagnetic atoms and molecules [6–11]. This method has previously been employed to load cold hydrogen (H) atoms in a magnetic trap [12]. The present article describes the Zeeman deceleration and magnetic trapping of deuterium (D) atoms.

The production of cold samples of hydrogen and its isotopes represents a considerable experimental challenge. The work of Silvera and Walraven (University of Amsterdam) [13,14] and Kleppner, Greytak, and coworkers (MIT) [15,16] has demonstrated the possibility of producing low-temperature samples of H in cryogenic cells, the inner walls of which are coated with ^{3}He-^{4}He mixtures [17,18]. The Amsterdam group has demonstrated laser cooling of H atoms to the recoil limit at a temperature of 3 mK [19]. The experimental efforts at MIT have culminated in the observation of a Bose-Einstein condensate (BEC) of H [20].

Extending these techniques to the production of cold D atoms has proven extremely difficult, primarily because the larger binding energy of D to the helium film on the inner surface of the cells leads to recombination losses [21–25]. For this reason, it has not been possible so far to trap cold samples of D atoms. We describe here an alternative route, based on multistage Zeeman deceleration, to produce and trap D atoms at a temperature of ~100 mK. This new method may find applications in precise measurements of fundamental frequency intervals in D [26,27] and may also represent a first step toward reaching quantum degeneracy in this fundamental atomic system. As this approach is also suited to produce cold stationary samples of T, a possible measurement of the neutrino rest mass has been envisaged [9].

The multistage Zeeman decelerator used in the present experiments is an extension of the decelerator described in Ref. [12]. The instrument consists of three main parts [see Fig. 1(a)]: (i) a source chamber, (ii) a 24-stage decelerator, and (iii) a magnetic quadrupole trap. A pulsed supersonic beam of D atoms is produced by 193-nm excimer-laser photolysis of ND_3 (Linde Gas, purity, 99%) seeded in Kr (mixing ratio, 1:9), in a quartz capillary mounted on the base plate of a pulsed valve (Even-Lavie Type E.L.-5-2005 [28]). A skimmer (diameter, 2 mm) separates the source chamber from the decelerator.

The decelerator consists of two sections each containing 12 solenoids made of 400-μm-diameter copper wire (inner diameter, 7 mm; 64 windings; four layers; current, 300 A; maximal magnetic field on axis, 2.2 T; see [12]) wound on the outside of a quartz tube through which the gas beam propagates. These two sections are separated by a 9-cm-long pumping region equipped with two coaxial collimating solenoids [see Fig. 1(a)]. These solenoids are composed of 66 windings of enameled copper tubing (1 mm in outside diameter, 600 μm in inside diameter) wound in six layers and are cooled with a constant flow of deionized water through the copper tubing. The innermost layer is wound at a radius of 6 mm and the distance between the centers of the two solenoids amounts to 28 mm. These solenoids are connected in series and pulsed with a current of 240 A during the time the atoms pass from the first section of the decelerator to the second, and they also provide a background magnetic field to maintain a quantization axis for the decelerating bunch of D atoms [7].

At the end of the decelerator, a magnetic quadrupole trap consisting of two coaxial solenoids with centers separated by 24 mm is mounted. With the exceptions of a smaller inner radius of the solenoids of 4 mm and a higher number of windings of 84, they are similar to those used between the two decelerator sections. When pulsed with currents of 200 A, these solenoids produce a maximal magnetic field strength on axis of 1.0 T and the lowest saddle point of the quadrupole trap results in a trap depth of 120 mK for D atoms.

Deuterium atoms are detected by photoionization at the trap center [see Fig. 1(a)] using a frequency-doubled pulsed dye laser (243 nm) in a 2+1 resonance-enhanced three-photon ionization sequence via the 2S state. The ions are extracted along the decelerator axis by applying a pulsed electric field of 1.4 kV/cm and 300 ns in duration immediately after the laser pulse and are detected on a microchannel plate detector (MCP) located 17 cm from the ionization point. Time-of-flight (TOF) profiles of the decelerated and trapped atoms are measured by varying the delay between the production of the D atoms with the excimer laser and their ionization with the 243-nm laser.

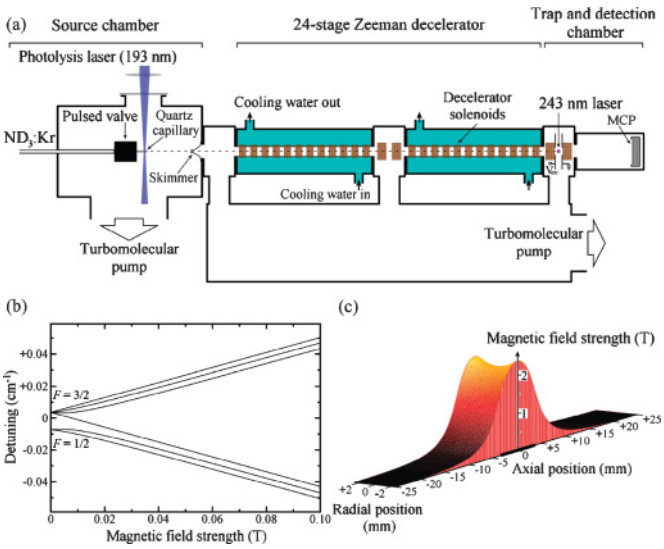

FIG. 1. (Color online) (a) Twenty-four stage Zeeman decelerator and magnetic trap for D atoms generated by photolysis in a pulsed supersonic expansion. (b) The Zeeman effect in the ground state of D. (c) Magnetic-field distribution in a single decelerator solenoid operated at 300 A.

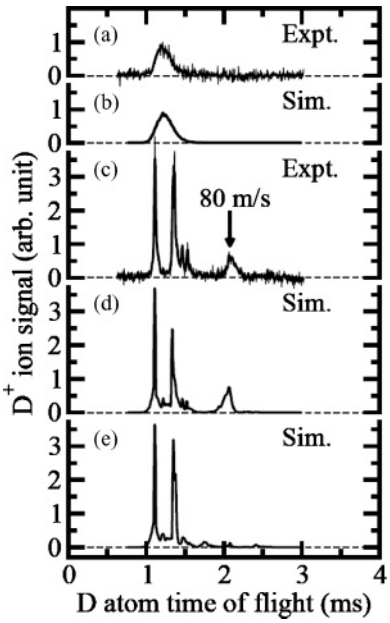

FIG. 2. TOF profiles of D atoms initially moving in a pulsed supersonic beam with a mean velocity of 475 m/s. The experimental trace obtained without turning the decelerator on and its simulation are displayed in panels (a) and (b), respectively. Panels (c) and (d) show the TOF profile recorded with an improved magnetic field pulse sequence and its simulation, respectively. Panel (e) represents a simulated TOF profile for a deceleration pulse sequence with a constant nominal phase angle of 24°. The intensity scales of panels (a) and (c) are identical.

The decelerator is operated to slow down D atoms in low-field-seeking Zeeman levels, that is, levels the energy of which increases with increasing magnetic fields [see Fig. 1(b)]. Such atoms gain potential energy and thus lose kinetic energy as they enter each solenoid. The deceleration principle has been described in detail in Ref. [7] and is only briefly summarized here. The supersonic beam is slowed down by applying sequences of pulsed currents to the solenoids that are designed to achieve a phase-stable deceleration in both the longitudinal and the transverse directions. As explained in Ref. [10], the sequences are precalculated using a three-dimensional particle-trajectory simulation program. The pulse sequences are specified by the times the current pulses in the solenoid are switched off and are given as phase angles defined for the synchronous particle with respect to the center of the active solenoid (see Fig. 1 of Ref. [7]). Because of the finite fall times of ~8 μs of the current pulses, the atoms can travel up to 4 mm along the decelerator axis before the current has returned to zero. Consequently, the effective phase angle is larger than the nominal phase angle that specifies the onset of the switch-off of each pulse.

An aspect of the radial magnetic-field distribution of the solenoids that is important for the present study is the fact that the radial field is maximal on axis in the regions of low magnetic fields outside the solenoids, but minimal in regions of high magnetic fields inside the solenoids [see Fig. 1(c)]. Consequently, solenoids operated at low phase angles exert smaller transverse forces than those operated at high phase angles.

Figure 2 illustrates the results of TOF measurements carried out with the decelerator described previously. Figure 2(a) shows the D-atom TOF distribution obtained without turning the decelerator on and provides information on the velocity distribution of the D atoms in the pulsed supersonic beam. The atoms reach the detection region after a time of flight of approximately 1.2 ms. The simulation of the experimental trace depicted in Fig. 2(b) was obtained by considering the geometrical constraints imposed by the long decelerator tube, which are more stringent than those imposed by the skimmer opening. The experimental data are best described by assuming that the D atoms initially move with a mean initial velocity of 475 m/s and that the velocity distribution corresponds to a Gaussian with an 80 m/s (4 m/s) full width at half maximum in the longitudinal (transverse) dimensions.

While designing deceleration pulse sequences by simulation prior to the experiments it was found that operating the decelerator at the constant phase angle of 24° that would be required to slow down the D atoms to final velocities below 100 m/s in 24 stages leads to a very low number of decelerated particles. This behavior, which is caused by transverse focusing or defocusing effects, is illustrated by the simulation trace depicted in Fig. 2(e). This trace is dominated by two strong early TOF peaks corresponding to atoms guided through the decelerator at almost constant speed, as explained in Ref. [10], and exhibits very little signal from low-velocity atoms, expected to arrive at ~2.1 ms. A considerably more intense beam of slow atoms could be achieved with pulse sequences that start with low-phase-angle pulses (~20°) and end with higher-phase-angle pulses (~55°) and which include several high-phase-angle pulses (~140°). With such pulse sequences, the number of decelerated particles can be enhanced by a factor of more than 10 without significant broadening of the velocity distribution, as is illustrated in Fig. 2(d). This simulation was obtained using the sequence

($5 \times 20°$, 140°, 35°, $7 \times 20°$, 140°, 45°, 50°, 140°, $3 \times 45°$, $3 \times 55°$) of phase angles for the 24 pulses, which was found to be very efficient for the deceleration of D atoms from an initial velocity of 475 m/s to a final velocity of 80 m/s. Each of the solenoids operated at high phase angle fulfills the purpose of rapidly refocusing diverging components of the decelerated bunch of atoms. The high-phase-angle stages at the end of the decelerator are needed so that the main deceleration is achieved over as short a time and as short a distance as possible, and they also enable efficient longitudinal focusing in the vicinity of the trap minimum [29,30]. The experimental trace displayed in Fig. 2(c) was measured using the deceleration pulse sequence described previously. The agreement between the experimental and simulated traces confirms the efficiency of this pulse sequence: The final velocity of the decelerated atoms is 80 m/s, and the peak intensity corresponds to that of the undecelerated beam at the end of the decelerator [compare with Fig. 2(a)]. Deuterium-atom beams with velocities below 100 m/s can be efficiently loaded into a magnetic trap if the trap loading process is carefully optimized.

As described in Ref. [12], the trap loading takes place in three steps: (i) deceleration with the first trap solenoid, (ii) stopping the slow beam with the second trap solenoid, and (iii) trapping by inverting the direction of current flow in the first trap solenoid. The optimal trap loading is achieved by bringing the atoms to a standstill at the center of the trap where the detection laser intersects the beam propagation axis. In this way, oscillations in the trap are reduced and minimal heating of the atom cloud results.

Experimentally, the optimal trap loading conditions are obtained by monitoring the decelerated atoms passing the detection region, first in the forward direction and then, after reflection, in the backward direction and by minimizing the time between the corresponding TOF peaks. The procedure is illustrated in Fig. 3. The last two TOF peaks in the experimental and simulated traces in panels (a) and (b) correspond to atoms moving forward and backward through the detection region. The velocity of the atoms moving forward is 30 m/s (20 m/s) for the conditions used to record the TOF trace in panel (a) [panel (b)], as determined from the simulations. In the experiment, the velocity is varied by adjusting the switch-off time of the first trap solenoid, higher velocities being achieved with earlier switch-off times. The trace in Fig. 3(c) shows only one main peak, indicating that the atoms are stopped at the detection point in the middle of the trap. When this situation is reached, the trap can be closed. The simulations, in the right-hand column of Fig. 3, provide information on the velocity distributions of the atoms contributing to the TOF peaks and clearly illustrate the behavior described earlier. Note that the early peaks (at 2.0 ms) in the experimental traces, which are also visible in the simulated traces, originate from a small bunch of faster atoms that cannot be reflected with the applied field gradients.

In Fig. 4 the trapping of D atoms monitored after optimal trap loading [corresponding to Fig. 3(c)] is compared with the trapping achieved under the conditions depicted in Fig. 3(a). In the former case, Fig. 4(a), the atoms are focused once (at ~2.8 ms) after the trap is switched on and the TOF trace hardly shows any subsequent structure. In the latter case, Fig. 4(c), strong oscillations are observable and the trapping

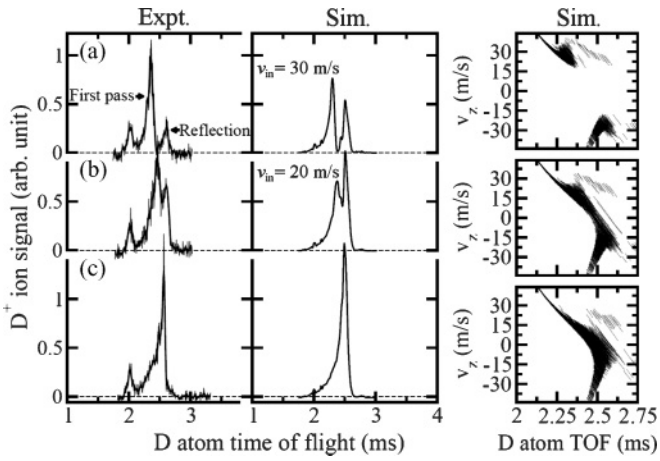

FIG. 3. Determination of optimal trap loading conditions. In panels (a) and (b) the D atoms enter the trap with too high a velocity ($v_{in} = 30$ m/s and $v_{in} = 20$ m/s, respectively), pass the detection region, and are reflected by the back wall of the trap. In (c) the initial velocity is reduced so that the atoms are stopped in the middle of the trap. The experimentally measured TOF distributions (Expt., left-hand column) are compared with the results of particle-trajectory simulations (Sim., middle column) from which the velocity distributions during the reflection process displayed in the three corresponding panels in the right-hand column were extracted. The intensity scales of the three experimental traces are identical.

efficiency is dramatically reduced. In Fig. 4(a) the decay of the D-atom signal beyond 4 ms originates from the gradual discharge of the capacitors used to maintain the current in the trap solenoids. In future experiments, this effect can be avoided by modifying the switching electronics.

The simulation of the experimental trapping measurement displayed in Fig. 4(a) is illustrated in Fig. 4(b) and captures the main features of the experimental trace very reliably. The

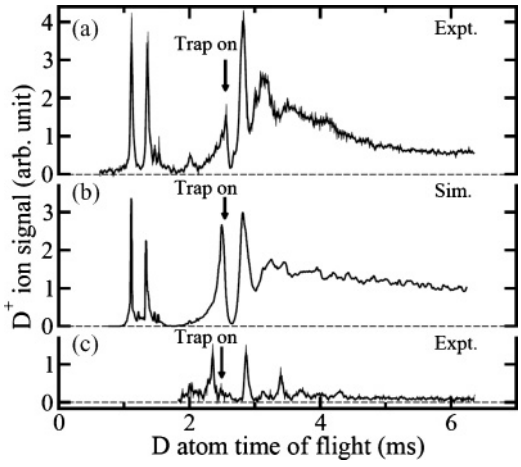

FIG. 4. Trapping D atoms. The experimental and simulated profiles obtained for the optimal trap loading condition corresponding to Fig. 3(c) are displayed in panels (a) and (b), respectively. For comparison, the experimental D-atom TOF profile recorded under conditions corresponding to Fig. 3(a) is shown in panel (c). Up to 2.5 ms, the signal corresponds to D atoms passing through the detection point without being trapped. After 2.5 ms, it corresponds to the density of trapped atoms in the ionization volume. The intensity scales of panels (a) and (c) are identical.

agreement between simulation and experiment enables the characterization of the deceleration and trapping process and the extraction of information on the velocity distribution of the trapped atoms and thus on the temperature of the trapped sample. Analyzing the velocity distribution of the atoms in the trap at 4 ms, when the amplitude in the oscillation of the signal strength is no longer observable, enables us to estimate the temperature of the trapped atom cloud to be $\sim$100 mK. From the beam waist of the detection laser in the center of the trap, the known 1S-2S two-photon absorption and ionization cross sections, and the magnitude of the detected D^+ ion signal, we determine the density of trapped atoms to be $\sim 10^6\,\mathrm{cm}^{-3}$.

In conclusion, a method to efficiently load a magnetic tap at the end of a multistage Zeeman decelerator without inducing undesirable heating of the trapped atoms has been presented. The method is similar to that described previously by Bethlem *et al.* [3] for an electrostatic trap. A sequence of pulsed currents applied at irregular phase angles has been employed to efficiently produce slow beams of D atoms. Quantitative agreement with the experiment has been achieved in simulations of the trap loading process, a notoriously difficult task. Figure 4 illustrates our ability to fully characterize the operational principles of our multistage Zeeman decelerator and the trapping procedure. These results also represent a demonstration of trapping D atoms, which had not been possible previously.

This work was supported by the Swiss National Science Foundation under Project 200020-122128, the ERC advanced grant program (Grant No. 228286), and the QSIT initiative of ETH.

[1] H. L. Bethlem, G. Berden, and G. Meijer, Phys. Rev. Lett. **83**, 1558 (1999).

[2] H. L. Bethlem, F. M. H. Crompvoets, R. T. Jongma, S. Y. T. van de Meerakker, and G. Meijer, Phys. Rev. A **65**, 053416 (2002).

[3] H. L. Bethlem, G. Berden, F. M. H. Crompvoets, R. T. Jongma, A. J. A. van Roij, and G. Meijer, Nature (London) **406**, 491 (2000).

[4] J. van Veldhoven, H. L. Bethlem, and G. Meijer, Phys. Rev. Lett. **94**, 083001 (2005).

[5] B. C. Sawyer, B. L. Lev, E. R. Hudson, B. K. Stuhl, M. Lara, J. L. Bohn, and J. Ye, Phys. Rev. Lett. **98**, 253002 (2007).

[6] N. Vanhaecke, U. Meier, M. Andrist, B. H. Meier, and F. Merkt, Phys. Rev. A **75**, 031402(R) (2007).

[7] S. D. Hogan, D. Sprecher, M. Andrist, N. Vanhaecke, and F. Merkt, Phys. Rev. A **76**, 023412 (2007).

[8] E. Narevicius, C. G. Parthey, A. Libson, J. Narevicius, I. Chavez, U. Even, and M. G. Raizen, New J. Phys. **9**, 358 (2007).

[9] E. Narevicius, A. Libson, C. G. Parthey, I. Chavez, J. Narevicius, U. Even, and M. G. Raizen, Phys. Rev. Lett. **100**, 093003 (2008).

[10] S. D. Hogan, A. W. Wiederkehr, M. Andrist, H. Schmutz, and F. Merkt, J. Phys. B **41**, 081005 (2008).

[11] E. Narevicius, A. Libson, C. G. Parthey, I. Chavez, J. Narevicius, U. Even, and M. G. Raizen, Phys. Rev. A **77**, 051401(R) (2008).

[12] S. D. Hogan, A. W. Wiederkehr, H. Schmutz, and F. Merkt, Phys. Rev. Lett. **101**, 143001 (2008).

[13] I. F. Silvera and J. T. M. Walraven, Phys. Rev. Lett. **44**, 164 (1980).

[14] I. F. Silvera and J. T. M. Walraven, *Progress in Low Temperature Physics*, edited by D. F. Brewer (Elsevier, Amsterdam, 1986), Vol. 10, p. 139.

[15] R. W. Cline, D. A. Smith, T. J. Greytak, and D. Kleppner, Phys. Rev. Lett. **45**, 2117 (1980).

[16] H. F. Hess, D. A. Bell, G. P. Kochanski, R. W. Cline, D. Kleppner, and T. J. Greytak, Phys. Rev. Lett. **51**, 483 (1983).

[17] H. F. Hess, G. P. Kochanski, J. M. Doyle, N. Masuhara, D. Kleppner, and T. J. Greytak, Phys. Rev. Lett. **59**, 672 (1987).

[18] R. van Roijen, J. J. Berkhout, S. Jaakkola, and J. T. M. Walraven, Phys. Rev. Lett. **61**, 931 (1988).

[19] I. D. Setija, H. G. C. Werij, O. J. Luiten, M. W. Reynolds, T. W. Hijmans, and J. T. M. Walraven, Phys. Rev. Lett. **70**, 2257 (1993).

[20] D. G. Fried, T. C. Killian, L. Willmann, D. Landhuis, S. C. Moss, D. Kleppner, and T. J. Greytak, Phys. Rev. Lett. **81**, 3811 (1998).

[21] I. F. Silvera and J. T. M. Walraven, Phys. Rev. Lett. **45**, 1268 (1980).

[22] R. Mayer and G. Seidel, Phys. Rev. B **31**, 4199 (1985).

[23] I. Shinkoda, M. W. Reynolds, R. W. Cline, and W. N. Hardy, Phys. Rev. Lett. **57**, 1243 (1986).

[24] T. Arai, M. Yamane, A. Fukuda, and T. Mizusaki, J. Low Temp. Phys. **112**, 373 (1998).

[25] A. P. Mosk, M. W. Reynolds, and T. W. Hijmans, Phys. Rev. A **64**, 022901 (2001).

[26] A. Huber, Th. Udem, B. Gross, J. Reichert, M. Kourogi, K. Pachucki, M. M. Weitz, and T. W. Hänsch, Phys. Rev. Lett. **80**, 468 (1998).

[27] N. Kolachevsky, P. Fendel, S. G. Karshenboim, and T. W. Hänsch, Phys. Rev. A **70**, 062503 (2004).

[28] M. Hillenkamp, S. Keinan, and U. Even, J. Chem. Phys. **118**, 8699 (2003).

[29] F. M. H. Crompvoets, R. T. Jongma, H. L. Bethlem, A. J. A. van Roij, and G. Meijer, Phys. Rev. Lett. **89**, 093004 (2002).

[30] L. P. Parazzoli, N. Fitch, D. S. Lobser, and H. J. Lewandowski, New J. Phys. **11**, 055031 (2009).